Biophysical Chemistry 11 (1980) 377–386

KINETICS OF HELIX–COIL TRANSITION OF POLYPEPTIDES IN SOLUTION BY THE RELAXATION METHODS

Takayuki SANO and Tatsuya YASUNAGA
Department of Chemistry, Faculty of Science, Hiroshima University, Hiroshima 730, Japan

Relaxation phenomena were studied in aqueous solutions of poly (α-L-glutamic acid) $(Glu)_n$ and poly (α-L-lysine) $(Lys)_n$ under various conditions using the electric field pulse method with detection by conductivity change. The relaxation time for the $(Glu)_n$ has a maximum value at the midpoint of the helix–coil transition. Some possible mechanisms are discussed and the observed relaxation phenomenon is attributed to the helix–coil transition. In the case of $(Lys)_n$, the relaxation time as a function of pH exhibits two maxima. One is assigned to a proton transfer reaction and the other to the helix–coil transition. Using the Schwarz's theory the rate constants of the helix growth step for both $(Glu)_n$ and $(Lys)_n$ are estimated. The difference in the activation parameters for $(Glu)_n$ and $(Lys)_n$ is discussed.

1. Introduction

The conformational transitions of biopolymers are known to play an important role in their functions in biological systems. The helix–coil (H–C) transition of synthetic polypeptides has been studied extensively as a useful model for conformational transitions of biopolymers. The equilibrium properties of the H–C transition have been studied in detail both experimentally and theoretically [1]. Many kinetic studies have been made by the various relaxation methods such as the temperature-jump [2,3], ultrasonic absorption [4–7], and dielectric relaxation techniques [8,9]. However, the dynamic features of the H–C transition still are not clear.

Burke et al. have estimated limits for the relaxation time of the H–C transition of $(Glu)_n$ as $5 \times 10^{-8} < \tau < 10^{-5}$ by combining their result of ultrasonic absorption with that of the temperature-jump method by Lumry et al. [2]. Subsequently, relaxation phenomena due to H–C transitions have been observed experimentally by using the ultrasonic absorption method for poly(α-D-glutamic acid) by Inoue [6] and for $(Glu)_n$ by Barksdale et al. [7]. The maximum relaxation times near the midpoint of the H–C transition have been estimated as 1.1×10^{-6} s at 30°C and 1×10^{-6} s in 0.03 M NaCl at 37°C, respectively.

On the other hand, for aqueous $(Lys)_n$ which differs from $(Glu)_n$ in chain length and the kind of dissociating groups, relaxation due to the H–C transition has not yet been observed. Only the relaxation of the proton transfer process by ultrasonic absorption measurement has been found [10].

The purpose of the present work is to confirm the assignment of the relaxations observed by the electric field pulse (EFP) method and to obtain the detailed information of the dynamic picture for the H–C transition of the $(Glu)_n$ and $(Lys)_n$.

2. Experimental

The sodium salts of $(Glu)_n$, $(NaGlu)_n$, with degrees of polymerization (dp) of 100, 250, and 700 were supplied from Ajinomoto Co., Inc. The samples were dialyzed against deionized water for 2 days and lyophilized and dried at 50°C for 4 hr in a vacuum just prior to the preparation of the stock solutions (5×10^{-4} residue mole) which were stored in a refrigerator. The sample solutions were prepared by dilution of the stock solution with deionized, distilled water to the desired concentration. Since low conductivity of the solution is required for the EFP measurements in order to obtain a square wave pulse, the concentration range used is limited from 5×10^{-5} to 2×10^{-4} residue mole. The tetrabutylammonium salt of $(Glu)_n$, $(TBAGlu)_n$ was

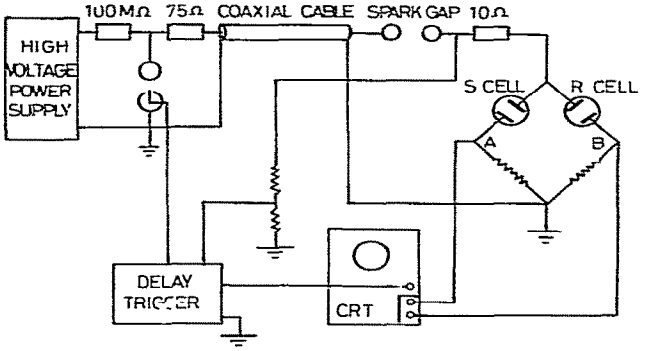

Fig. 1. The block-diagram of the electric field pulse apparatus.

prepared by passing a given volume of $(NaGlu)_n$ solution through the column of TBA-neutralized cation-exchange resin (Dowex 50 W-X8). Completeness of ion exchange was checked by flame test. For pH adjustment, HCl, NaOH, and tetrabutylammonium hydroxide were used. All these chemicals were of reagent grade and were used without further purification. Hydrobromide salt of $(Lys)_n$, $(LysHBr)_n$, was purchased from the Protein Research Foundation, Japan. The samples were dialyzed against deionized and carbon dioxide-free water. Three different sample solutions were obtained through dialysis and ultrafiltration: low (degree of polymerization, DP, 90), middle (DP 300), and high ($DP \gg 300$). Molecular weights were determined by sedimentation velocity measurement using the HITACHI UCA-1A ultracentrifuge. The poly (L-lysine hydroxide), $(LysHOH)_n$, and poly(L-lysine acetate), $(LysHAc)_n$, solutions were prepared by passing $(LysHBr)_n$ through a column of anion-exchange resin, Amberlite 400. The pH indicators were of reagent grade and were used without further purification. The pH measurements were carried out with an accuracy of ±0.05 pH unit by a Hitachi-Horiba F-5 type pH meter at room temperature just before the relaxation studies and the optical rotatory dispersion (ORD) measurements. In order to obtain the degree of dissociation, α, the titration of $(Glu)_n$ and $(Lys)_n$ solutions was performed with HCl or NaOH at room temperature in a nitrogen atmosphere. To avoid a large error resulting from a change in the pH value which is due to contamination by KCl from the calomel electrode during the course of the usual titration, pH measurements were carried out on a very small amount of solution taken from the large quantity of the titrated sample solution. The degree of dissociation was calculated as a function of pH by subtracting the black curve graphically from the curve of the $(Glu)_n$ and $(Lys)_n$ solution, respectively.

ORD measurements were carried out in the wavelength 225–350 nm with a JASCO ORD/UV-5 spectropolarimeter using a 5-cm quartz lidded cell. The temperature was controlled to ±0.2°C by circulating thermostated water around the cell. The helix contents were evaluated from ORD data using the following equation

$$\theta = \frac{[m']_{\lambda_0} - [m']^{c}_{\lambda_0}}{[m']^{h}_{\lambda_0} - [m']^{c}_{\lambda_0}} , \tag{1}$$

where $[m']_{\lambda_0}$ is the measured value of the reduced residue rotation at the minimum point of the trough in the vicinity of 233 nm, and $[m']^{h}_{\lambda_0}$ and $[m']^{c}_{\lambda_0}$ are the reduced residue rotations for completely helical and coiled states, respectively. These values were calculated from the following equations by Warashina and Ikegami [11] as a function of temperature T (°C) for $(Glu)_n$

$$[m'(T)]^{h}_{233} = -18400 + 66T , \tag{2}$$

$$[m']^{c}_{233} = -2000 , \tag{3}$$

and by Chou and Scheraga [12] for $(Lys)_n$

$$[m'(T)]^{h}_{233} = -16200 + 100T , \tag{4}$$

$$[m']^{c}_{233} = -2200 . \tag{5}$$

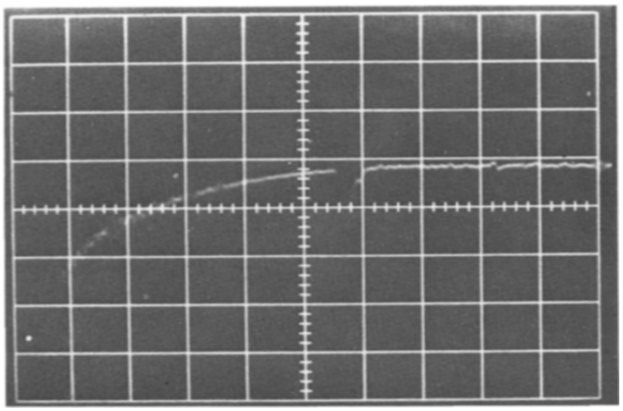

Fig. 2. The typical relaxation spectrum for $(NaGlu)_n$ (DP = 250), 1.0×10^{-4} residue mole, pH 6.63, at 25°C; sweep 2 μs/div. [33].

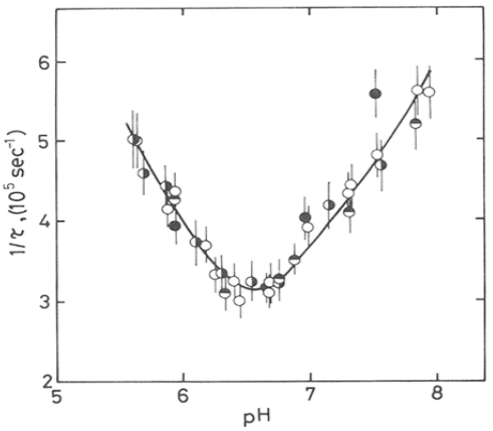

Fig. 3. The concentration dependence of the reciprocal relaxation time versus pH curve for $(NaGlu)_n$ (DP = 250) at 25°C. (◑) 5.7×10^{-5} residue mole, (◒) 8.0×10^{-5} residue mole, (○) 1.0×10^{-4} residue mole, (●) 2.0×10^{-4} residue mole [33].

The electric field pulse apparatus used here is similar to that originally constructed by Ilgenfritz [13]. A block diagram of the apparatus is shown in fig. 1. A 1-km length of 10C-2V coaxial cable was used as a capacitor. The transients were followed by monitoring the conductance change with a Wheatstone bridge. The difference in voltage between points A and B (fig. 1) was detected by a Tektronix type W plug-in differential preamplifier. Two resistances of the lower arms of the bridge are equal and the value of resistance is selected so as to give about 10 V as input signals of the amplifier. The distance between the two electrodes of the sample cell is fixed at 0.3 cm and that of the reference cell is kept variable. The reference cell contains a NaCl solution of approximately the same conductance as the sample solution. The resistances of both cells were matched precisely by adjusting the distance of the two electrodes of the reference cell. The duration of the high voltage pulse applied to the bridge is 10 or 20 μs, and the rise and decay times of the applied electric field are much faster than 0.1 μs. The electric field intensity in the cell is usually about 30 kV/cm. As a test of the apparatus, dissociation field effects for two pH indicators, bromcresol purple and phenol red, were measured spectrophotometrically, and the results agreed with those reported by Ilgenfritz [13].

3. Results and discussion

3.1. Poly(α-L-glutamic acid)

The kinetic measurements were carried out in the pH range 5.5–8.0. Outside this pH range there still existed a small amplitude relaxation for which an accurate relaxation time could not be estimated because of its small magnitude, and at the extremes of pH 5.0 and 9.0 the relaxation effect disappeared completely. A typical relaxation curve is shown in fig. 2. The direction of the relaxation signal indicates an increase in the conductance of the solution by the application of the electric field. The relaxation spectra show that a rapid increase of conductance occurs with application of the electric field and is followed by the relaxation part of the conductance increase, which is characterized by a single relaxation at all pH values. Fig. 3 shows the pH dependence of the relaxation time for $(NaGlu)_n$ with dp = 250 at various polymer concentrations (5×10^{-5} –2×10^{-4} residue mole). The relaxation time has a maximum value at pH 6.6 and is independent of polymer concentration. Fig. 4 shows the corresponding pH dependence of the helix content from the ORD measurements. In this figure the H–C transition region shifts considerably to the higher pH side in comparison with that reported in the literature [11,14,15] and depends slightly on the polymer concentration. These shifts of

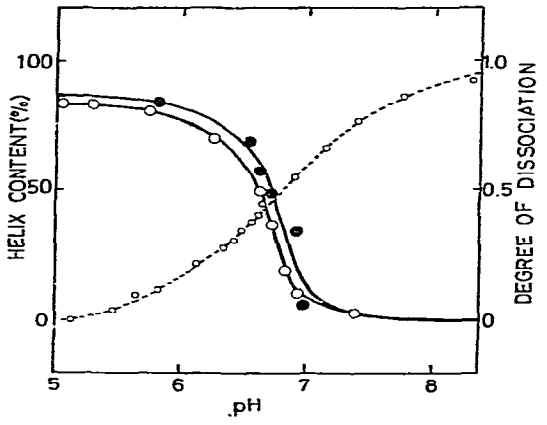

Fig. 4. The pH dependencies of the helix content (solid curve) and the degree of dissociation (dashed curve) for $(NaGlu)_n$ (DP = 250). Solid curve: (•) 5.0×10^{-5} residue mole, (○) 1.0×10^{-4} residue mole, at 25°C. Dashed curve: 1.0×10^{-4} residue mole at room temperature.[33].

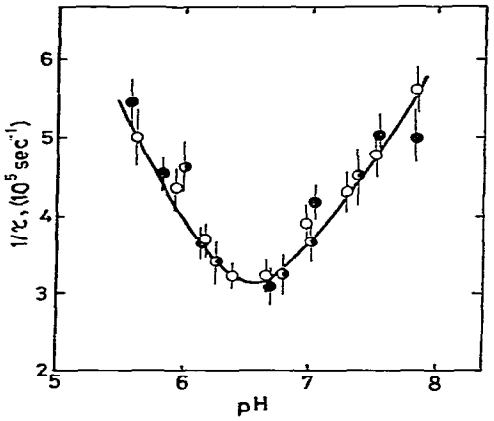

Fig. 5. The dependence of the reciprocal relaxation time versus pH curve on the electric field density for $(NaGlu)_n$ (DP = 250), 1.0×10^{-4} residue mole, at 25°C. (◑) 23 kV/cm, (○) 30 kV/cm, (•) 66 kV/cm [33].

the transition region can be explained as the effect of the ionic strength of the counterion [16]. It is seen from figs. 3 and 4 that the relaxation time reaches its maximum value in the vicinity of the midpoint of the H–C transition. This maximum at the midpoint of H–C transition was observed at all studied temperatures. The same results were obtained not only in the solution of $(TBAGlu)_n$ with dp = 250 but also in the solution of $(NaGlu)_n$ with dp = 700. However, in $(Glu)_n$ with lower dp (about 100) the magnitude of the relaxation was so small that accurate estimation of the relaxation time was not possible. Fig. 5 shows the pH dependence of the relaxation time under various electric field densities (EFD). Although a definite increase in the relaxation amplitude with EFD was observed on the experiments, the relaxation time remained constant as seen in fig. 5.

When a high electric field is applied to the polyelectrolyte solution, the conductivity may be affected in three different ways [17,18]. One of them is due to the change in mean mobility of the charge carriers caused by orientation of the long axis of the polyion in the direction of the field (orientational field effect). The second case is the increase in conductivity due to increased dissociation of the proton of the carboxyl group in the side chain or counterion bound to the polyion by application of a high electric field (dissociation field effect). Also there is the possibility that a high electric field induces the change in polyion mobility. Accordingly there exist four possible mechanisms for the observed relaxation processes: an orientation process, an ion-binding reaction of the counterion, the proton-transfer reaction, and the H–C transition. These possible mechanisms will be examined in detail.

3.1.1. Orientation field effect [17,18]

The electric field induces electric dipoles on the polyelectrolyte particles due to the polarization of the inner ionic atmospheres of the polyions and causes the orientation of their long axis in the direction of the field. As a consequence of anisotropy of the nonspherical particle, anisotropy of the conductivity is produced in the solution. When the orientation is caused by a pure induced dipole, which may be applied to the present case, the relaxation time of the orientation process at high EFD [17] is

$$\tau_E = 1.68 \times kT/\alpha_{11} D_r \times E^{-2} , \qquad (6)$$

where τ_E is relaxation time, α_{11} is polarizability perpendicular to the electric field, D_r is the rotational diffusion coefficient, and E is the electric field density, respectively. The most characteristic property of this equation is that τ_E is inversely proportional to the square of EFD. This is not consistent with the observed results in which the relaxation time is independent of

applied EFD. Furthermore, our preliminary experiments of electric birefringence show that the rise time of the electric birefringence is two times faster than the present relaxation time and decreases with EFD. These facts indicate that the present relaxation phenomena cannot be ascribed to the orientation field effect.

3.1.2. Ion binding process of the counterion

In a solution of polyelectrolyte, the counterion is bound around the polyion in two ways [19]. One is the specific association between counterions and the ionic groups of the polyion (site binding). The other is the association of the counterion in the vicinity of the polyion due to its large electrostatic field (ionic atmosphere binding). The application of the external field may bring about the removal of these counterions from the polyion, which leads to an increase in the conductance of the solution. The former type of binding, however, can be eliminated from the possible mechanisms by the experimental fact that no relaxation behavior changed when the counterion was converted from sodium to tetrabutylammonium ion, which is not site bound because of its large radius [19,20]. The latter mechanism is also not likely to be responsible for the observed relaxation due to the following considerations. The relaxation time for this process must be closely connected with the mobility of the counterion or the environment on the polyion. Accordingly, the relaxation behavior would be expected to change when the counterion is converted from sodium to tetrabutylammonium because of the difference in mobilities of both counterions. This speculation contradicts the observed behavior. Wissbrun et al. [21] also have studied conductance changes under high electric fields for polyacrylic acid and polystyrenesulfonic acid, etc., and assigned it to the reaction associated with removal of the counterion in the ionic atmosphere by application of the external field. In their experiments, the relaxation time showed no discernible variation with degree of dissociation but decreased with increasing electric field. They have also suggested that the relaxation time increases with molecular weight. These features of the relaxation time are opposite to the present relaxation phenomena. Thus the ion-binding reaction of the counterion also can be eliminated from the possible mechanisms.

Table 1
The maximum relaxation times $1/\tau_{max}$, and the rate constants, k_f, of the helix growth process for $(Glu)_n$ at various temperatures. In the estimations of k_f, σ value of 3×10^{-3} was used

T (°C)	$1/\tau_{max}$ (10^5 s^{-1})	k_f (10^7 s^{-1})
15	2.9 ± 0.2	2.4 ± 0.2
25	3.1 ± 0.2	2.6 ± 0.2
35	3.5 ± 0.2	2.9 ± 0.2
45	4.1 ± 0.3	3.4 ± 0.2

3.1.3. Proton transfer reaction of the carboxyl group

For the following proton-transfer equilibrium of the carboxyl group in the side chain

$$RCOOH \underset{k_{-1}}{\overset{k_1}{\rightleftharpoons}} RCOO^- + H^+ , \qquad (I)$$

the relaxation time is expressed by the following equations

$$1/\tau = k_{-1}[(RCOO^-) + (H^+)] + k_1 , \qquad (7)$$

$$= k_{-1}[\alpha C_0 + (H^+) + K_{app}] , \qquad (8)$$

where α is the degree of dissociation in the carboxyl group, C_0 is the total polymer concentration, and K_{app} ($= k_1/k_{-1}$) is the apparent dissociation constant. The value of α obtained from the titration experiment is shown as a function of pH in fig. 4. In general, for the protolytic reaction the reciprocal relaxation time ($1/\tau$) has also the minimum value at a certain pH (pH_m), and pH_m is expected to be below 5.5 for the $(Glu)_n$. On the other hand, as the value of K_{app} is in the range 10^{-6}–10^{-7} in the present case, $\alpha C_0 + (H^+) > K_{app}$ is satisfied. Therefore the reciprocal relaxation time must increase monotonically with total polymer concentration at constant pH and with pH at constant polymer concentration. This expectation contradicts the present results in which the relaxation time does not show any discernible variation with polymer concentration and reaches its maximum value at pH 6.6. This fact indicates that the observed relaxation phenomena cannot be attributed directly to the proton-transfer reaction.

4.1.4. H–C transition

The observed relaxation phenomena cannot be explained by the above three mechanisms but can be satisfactorily explained with the H–C transition mechanism

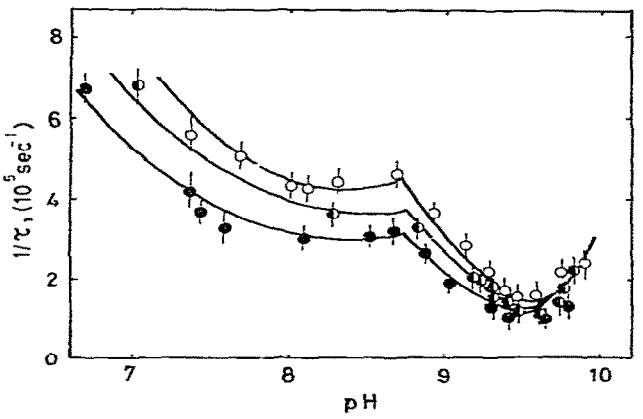

Fig. 6. Concentration dependence of the reciprocal relaxation time versus pH for $(LysHOH)_n$ at 19°C, (○) 2×10^{-4}, (●) 1×10^{-4}, and (●) 5×10^{-5} residue mole [34].

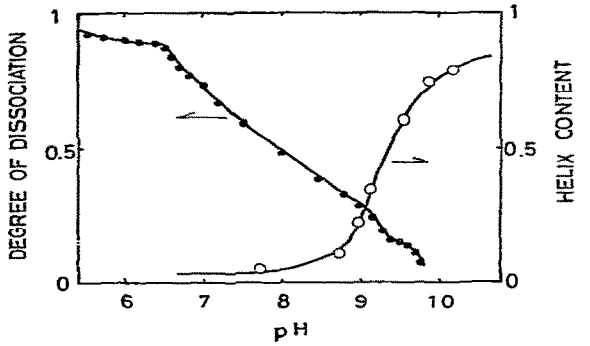

Fig. 7. The pH dependencies of the helix content (○) and the degree of dissociation (●) for $(LysHBr)_n$, 2×10^{-4} residue mole [34].

as will be shown below. The relaxation time goes through its maximum value in the midpoint of the transition and is independent of polymer concentration, kind of counterions, and applied EFD. These features of the relaxation time are easily understood in light of the H–C transition mechanism. Schwarz [22] has adapted the Zimm–Bragg model [23] to the kinetic theory of H–C transitions. According to his theory, the mean relaxation time of the H–C transition in the vicinity of the midpoint of the transition is expressed by the following equation

$$1/\tau = k_f[(s'-1)^2 + 4\sigma] , \qquad (9)$$

where k_f and s' are the forward rate constant and the equilibrium constant for the helix growth, respectively, and σ is the nucleation parameter. This equation predicts that the mean relaxation time has its maximum value at the midpoint of the transition and is independent of polymer concentration. At the transition midpoint, s' becomes unity and the equation is simplified to

$$1/\tau = 4\sigma k_f . \qquad (10)$$

The value of σ is given as $(3 \pm 2) \times 10^{-3}$ for $(Glu)_n$ from the titration experiments by Snipp et al. [15] and is independent of ionic strength [15] and temperature [24]. Introducing the experimentally determined maximum relaxation times into the above equation, the rate constants of helix growth, k_f, are obtained at various temperatures and are given in table 1 where a σ value of 3×10^{-3} was used. These values are comparable to those obtained by other investigators, e.g., 4.4×10^7 s^{-1} for poly(α-D-glutamic acid) at 30°C by Inoue [6] and $(8 \pm 5) \times 10^7$ s^{-1} for $(Glu)_n$ in 0.03 M NaCl at 37°C by Barksdale et al. [7].

According to Eyring's absolute rate process, the rate constant k_f is related to the activation enthalpy $\Delta H^{\ddagger}$ and entropy $\Delta S^{\ddagger}$ as follows.

$$k_f = (kT/h)\exp\{-(\Delta H^{\ddagger} - T\Delta S^{\ddagger})/RT\} . \qquad (11)$$

The values of $\Delta H^{\ddagger}$ and $\Delta S^{\ddagger}$ were calculated to be 1.5 ± 0.4 kcal/mol and -20 ± 2 cal/mol, respectively, from a $\ln(k_f/T)$ versus $1/T$ plot. The small value of $\Delta H^{\ddagger}$ is to be expected for the H–C transition of polypeptides because it is connected mainly with the hydrogen bond formation which does not require any appreciable activation energy. However, an unexpectedly large value of $\Delta S^{\ddagger}$ cannot be explained by the diffusion-controlled formation of the hydrogen bond. Schwarz et al. [8] have estimated the maximum value of the relaxation time of poly(γ-benzyl L-glutamate) in a dichloroacetic acid-ethylene dichloride mixture as 5×10^{-7} s, which leads to a value for k_f of 1.3×10^{10} s^{-1}. This value of k_f shows that in the poly(γ-benzyl glutamate), the helix growth reaction must be practically diffusion controlled. Such differences in rate constants for the polypeptides with different side chains may be attributed to the nature of the interaction between the side chain and solvent. In the case of $(Glu)_n$, a large decrease of entropy in the activation state plays the important role in the H–C transition.

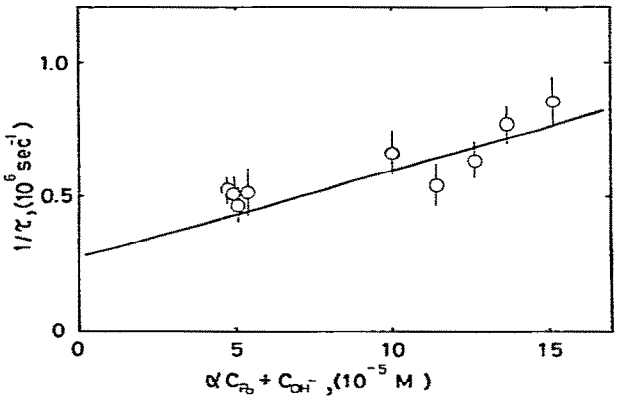

Fig. 8. Plot of concentration term in eq. (12) versus reciprocal relaxation time for $(LysHOH)_n$ at 22°C [34].

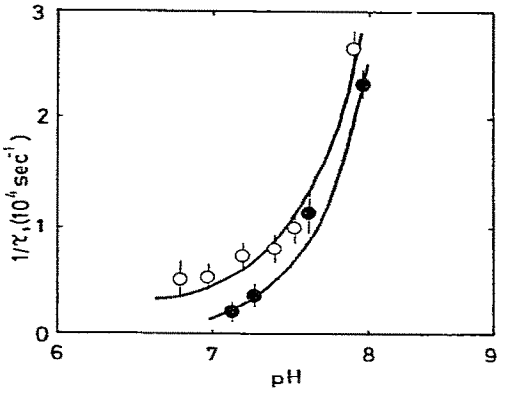

Fig. 9. The pH dependence of the reciprocal relaxation time for $(LysHBr)_n$-Neutral Red (•) and $(LysHAc)_n$-Neutral Red (○) system [34].

3.2. Poly (α-L-lysine)

Single relaxations were observed in the pH range 6.5–10, Fig. 6 shows the pH dependence of the reciprocal relaxation time for middle-DP$(LysHOH)_n$ at various polymer concentrations. The reciprocal relaxation time has two minima at the pH values where the degree of dissociation and the helical content are both nearly 0.5 (fig. 7). This result suggests that the relaxation phenomena in the high-pH region may be attributed to a helix-coil transition and in the low-pH region to a proton transfer reaction.

In order to clarify the relaxation mechanism in the low-pH region, a simple proton transfer reaction is considered

$$\mathrm{PH^+ + OH^- \underset{k_2}{\overset{k_1}{\rightleftharpoons}} P + H_2O}\,, \qquad \tau^{-1} = k_1(\alpha C_{po} + C_{OH^-}) + k_2\,, \tag{12}$$

where α is the degree of dissociation of the amino group and C_{po} is the total polymer concentration in residue mole unit. In fig. 8, τ^{-1} is plotted against $(\alpha C_{po} + C_{OH^-})$ as calculated from potentiometric titration data. According to eq. (12), the rate constant obtained for $(LysHOH)_n$ was $k_1 = (3 \pm 1) \times 10^9\ \mathrm{mol^{-1}\ s^{-1}}$. However, this reaction scheme for the proton transfer reaction may be somewhat oversimplified, since at neutral pH the observed relaxation time deviates from the calculated value.

To test more directly whether this relaxation is associated with a proton transfer, kinetic experiments with optical detection were performed on the pH indicator-$(Lys)_n$ system. Fig. 9 shows the pH dependence of the reciprocal relaxation time for the $(LysHBr)_n$- and $(LysHAc)_n$-Neutral Red systems, in which the intermolecular proton exchange reaction between polymer and indicator (Neutral Red) is considered in addition to the proton transfer reactions of the indicator and the polymer.

$$\begin{array}{ccc} \mathrm{InH^+ + OH^- + PH^+} & & \\ k_3 \swarrow\!\!\!\swarrow k_4 & & k_2 \nwarrow\!\!\!\nwarrow k_1 \\ \mathrm{In + PH^+ + H_2O} & \underset{k_6}{\overset{k_5}{\rightleftharpoons}} & \mathrm{InH^+ + P + H_2O} \end{array} \tag{13}$$

where In, InH^+ and P, PH^+ mean the unprotonated and protonated forms of the indicator and polymer side group, respectively. The reciprocal relaxation times for this scheme can be calculated from the following equation:

$$\begin{vmatrix} k_3(\mathrm{InH^+ + OH^-}) + k_6\mathrm{P} + k_5\mathrm{PH^+} + k_4 - \tau^{-1} & (k_3 - k_6)\mathrm{InH^+} - k_5\mathrm{In} \\ (k_1 - k_5)\mathrm{PH^+} - k_6\mathrm{P} & k_1(\mathrm{PH^+ + OH^-}) + k_5\mathrm{In} + k_6\mathrm{InH^+} + k_2 - \tau^{-1} \end{vmatrix} = 0 \tag{14}$$

The constants k_1 and k_5 were determined so as to obtain the best fit of the theoretical values of τ^{-1} to the experimental ones. In this procedure the dissociation constant of the indicator, Neutral Red, $pK_I = 6.7$ and

$k_3 = 2 \times 10^{10}\ s^{-1}\ M^{-1}$ were used, both taken from the literature [25]. The value of k_1 obtained for the indicator-$(Lys)_n$ systems was $(1.5 \pm 0.5) \times 10^9\ s^{-1}\ M^{-1}$. Recently, Zana and Tondre [10] have obtained the value of $7 \times 10^9\ s^{-1}\ M^{-1}$ for a proton transfer rate constant of $(LysHBr)_n$ by ultrasonic absorption measurement. These three values of k_1 agree with each other within an order of magnitude. This fact indicates that the relaxation phenomena in the low-pH region in fig. 6 can be attributed to a proton transfer reaction involving the amino groups of the polymer.

Next, we will focus on the relaxation phenomena in the high-pH region shown in fig. 6. Possible relaxation mechanisms are discussed below.

3.2.1. Dissociation field effects

If the relaxation is caused by the proton exchange reaction between $(Lys)_n$ and the hydroxide anion, the reciprocal relaxation time has to increase with pH near the transition region, according to eq. (12). This expectation is not consistent with the experimental results of the abrupt change in the relaxation time, despite taking into account the apparent dissociation constant.

In general, a counterion can associate with a side group of the polyion (site binding) or can bind to the polymer around its electrostatic field (ionic atmosphere binding). These binding equilibria can also be perturbed by the electric field and contribute to the change of conductivity in the solution. The kinetic aspect of the binding reaction of these equilibria, however, cannot be discussed precisely because of the lack of detailed information about these equilibria with respect to the kinds of counterions, such as acetate and bromide ions. Because of the present quantitative limitations, the estimation of the relaxation time depends on the electric field density for the atmosphere binding process. This dependences was not consistent with the experimental results. Furthermore, the relaxation time was shown to depend on the polymer concentration and the kind of counterion. These experimental facts seem to be consistent with the expectations for the site binding process. However, the pH dependence of relaxation time does not support a site binding process.

Consequently, these dissociation field effects can be eliminated from the possible mechanisms for the observed relaxation.

Table 2
Determination of the σ value from the sharpness of the transition and transition interval

Sample	ΔpH	$\Delta\alpha$	$\sigma^{-1/2}$	$\sigma \times 10^3$
$(LysHAc)_n$ [a]	1.7	0.09	11	7.7
$(LysHOH)_n$ [a]	1.3	0.05	27	1.4
$(LysHBr)_n$ [b]	1.3	0.06	22	2.0
$(LysHBr)_n$ [c]	0.71	0.14	20	2.5

a) 20°C; 2×10^{-4} residue mole.
b) 20°C; 3×10^{-4} residue mole.
c) 22°C; 1M KCl. From Barskaya and Ptitsyn, ref. [28].

3.2.2. Orientation field effects

Application of an electric field to a solution of polyion causes the shift of the ionic atmosphere on the polyion without dissociation, and then induces the orientation of the polarized polyion in the direction of the field. An anisotropy of the mobility of the polyions gives rise to an increase of conductivity in the parallel direction to the field and a decrease perpendicular to it. In this way, an intense electric field density brings about the conductivity change of solutions with the time constant defined by eq. (6). According to eq. (6), the relaxation time of the orientation process must be inversely proportional to the square of the electric field density and to the molecular weight. The observed result, however, is independent of applied electric field density and molecular weight. This fact indicates that the present relaxation phenomena cannot be attributed to the orientation field effects. Besides, polyelectrolytes such as $(Glu)_n$ and $(Lys)_n$ have such small permanent dipole moments compared to the induced dipole moment that the orientation field effect due to the permanent dipole moment can be eliminated from consideration. Other mechanisms, such as permanent and induced dipole polarization and Maxwell–Wagner effects, that have been investigated by the dielectric dispersion method [26,27] do not explain the observed relaxation, because these mechanisms give rise to a decrease in the conductivity. This contradicts the experimental results.

3.2.3. Helix–coil transition

None of the mechanisms discussed above can explain the relaxation phenomena in the high-pH region (fig. 6); thus only the helix–coil transition remains as a possible

Table 3
Rate constants of the helix growth process and activation parameters

Sample	$\Delta H^{\ddagger}$ (kcal mol^{-1})	$\Delta S^{\ddagger}$ (e.u.)	k_f (10^7 s^{-1})
$(LysHOH)_n$	13.3	10.1	1.9 a)
$(LysHBr)_n$	13.2	11.2	1.4 a)
$(LysHAc)_n$	12 4	6.8	0.36 a)
$(Glu)_n$	1.5	−10	2.6 b)

a) At 22°C. b) At 25°C.

mechanism. In order to calculate the k_f, according to eq. (10) the σ was obtained using the following relation proposed by Barskaya and Ptitsyn [24,28]

$$\sigma^{-1/2} = 4/2.3\,\Delta\mathrm{pH}\,\Delta\alpha\,, \qquad (15)$$

where $\Delta\alpha$ is a difference of the degree of dissociation between the helical and coiled states at the transition pH, and $\Delta\mathrm{pH} = (\mathrm{d\,pH/d}\theta)_{\theta=0.5}$ is the minimum transition interval (sharpness of transition). The σ values, along with those for $\Delta\alpha$ and ΔpH obtained graphically, are listed in table 2 for various $(Lys)_n$ salts.

Since the σ depends only slightly on the temperature [27,28] the temperature dependence of the relaxation time gives the activation parameters $\Delta H^{\ddagger}$ and $\Delta S^{\ddagger}$ for the helix growth process according to Eyring's equation. The results are listed in table 3, together with those for $(Glu)_n$. Though the values of k_f are comparable in magnitude, distinct differences in $\Delta H^{\ddagger}$ and $\Delta S^{\ddagger}$ exist between $(Lys)_n$ and $(Glu)_n$. The large positive values of $\Delta S^{\ddagger}$ and $\Delta H^{\ddagger}$ in comparison with those of $(Glu)_n$ cannot be discussed quantitatively at present, but may be interpreted as the effects of the longer side chain and the stronger interaction between side chain and solvent [29]. From these results, it can be deduced that the helix–coil transition of polypeptides is largely affected, not only by the charge condition of the dissociating groups, but also by the spatial location and the hydrophobic character of the side chain.

In general, the effects of the electric field on the helix–coil transition depend on the kinds of solvent and polypeptide, and cannot be described simply [30–32]. There are also two possible mechanisms for the electric-field-induced helix–coil transition in aqueous solutions of polypeptides:

1) transition induced by the difference of overall dipole moments between two conformations (dipole induced transition), and

2) transition induced by the repulsion of the dissociated side groups (charge-induced transition).

For $(Glu)_n$, unfortunately the relaxation associated with the proton transfer reaction could not be observed separately. Therefore it is difficult to distinguish definitely the two mechanism for the available data.

In the case of $(Lys)_n$, the relaxation time for H–C transition (at pH 9.0 ~ 9.5) depends on the polymer concentration, as can be seen in figure 6, which is not expected for the helix–coil transition. By considering the experimental results at a lower pH region, this fact can be interpreted by the coupling of the helix–coil transition with the faster and concentration-dependent process, namely, the dissociation reaction of side-chain groups. Therefore, the helix–coil transition of $(Lys)_n$ is induced through the second mechanism rather than the first one.

Acknowledgement

The authors thank the following for permission to use published material: the Editor of J. Am. Chem. Soc. for figures 2, 3, 4, 5 and John Wiley & Sons, Inc. for figures 6, 7, 8, 9.

References

[1] D. Poland and H.A. Scheraga, Theory of helix–coil transition in biopolymers (Academic, New York, 1970).
[2] R. Lumry, R. Leagre and W.G. Miller, Biopolymers 2 (1964) 489.
[3] E. Hamori and H.A. Scheraga, J. Phys. Chem. 71 (1967) 4147.
[4] R.C. Parker, L.J. Slutsky and K.R. Applegate, J. Phys. Chem. 72 (1968) 3177.
[5] G.G. Hammes and P.B. Roberts, J. Am. Chem. Soc. 91 (1969) 1812.
[6] H. Inoue, J. Sci. Hiroshima Univ. Ser A-2, 34 (1970) 37.
[7] A.D. Barksdale and J.E. Stuehr, J. Am. Chem. Soc. 94 (1972) 3334.
[8] G. Schwarz and J. Seelig, Biopolymers 6 (1968) 1263.
[9] A. Wada, T. Tanaka and H. Kihara, Biopolymers 11 (1972) 587.
[10] R. Zana and C. Tondre, J. Phys. Chem. 76 (1972) 1737.
[11] A. Warashina and A. Ikegami, Biopolymers 11 (1972) 529.
[12] P.Y. Chou and H.A. Sheraga, Biopolymers 10 (1971) 657.
[13] G. Ilgenfritz, Ph. D. Thesis, George August University, Göttingen (1966).

[14] M. Nagasawa and A. Holtzer, J. Am. Chem. Soc. 86 (1964) 438.
[15] R.L. Snipp, W.G. Miller and R.E. Nylund, J. Am. Chem. Soc. 87 (1965) 3547.
[16] H. Takesada, H. Yamazaki and A. Wada, Biopolymers 4 (1966) 713.
[17] M. Eigen and G. Schwarz, J. Colloid Sci. 12 (1957) 181.
[18] N. Ise, M. Eigen and G. Schwarz, Biopolymers 1 (1963) 343.
[19] U.P. Strauss and Y.P. Leung, J. Am. Chem. Soc. 87 (1965) 1476.
[20] R. Zana, J. Am. Chem. Soc. 94 (1972) 3646.
[21] K.F. Wissbrun and A. Patterson, Jr., J. Polym. Sci. 33 (1958) 235.
[22] G. Schwarz, J. Mol. Biol. 11 (1965) 64.
[23] B. Zimm and J. Bragg, J. Chem. Phys. 31 (1959) 526.
[24] V.E. Bychkova, O.B. Ptitsyn and T.V. Barskaya, Biopolymers 10 (1971) 2161.
[25] W.M. Clark and M.E. Perkins, J. Am. Chem. Soc. 54 (1932) 1228.
[26] M. Mandel, Mol. Phys. 4 (1961) 489.
[27] M. Mandel and A. Jenard, Trans. Faraday Soc. 59 (1963) 2158.
[28] T.V. Barskaya and O.B. Ptitsyn, Biopolymers 10 (1971) 2181.
[29] N. Murai and S. Sugai, Biopolymers 13 (1974) 1161.
[30] G. Schwarz, Biopolymers 14 (1975) 1173.
[31] C.P. Bean and A.J. Bennett, Biopolymers 12 (1973) 817.
[32] K. Kikuchi and K. Yoshioka, Biopolymers 15 (1976) 1669.
[33] Y. Tsuji, T. Yasunaga, T. Sano and H. Ushio, J. Am. Chem. Soc. 98 (1976) 813.
[34] S. Inoue, T. Sano, Y. Yakabe, H. Ushio and T. Yasunaga, Biopolymers 18 (1979) 681.